Synthesis, Structural Studies, and Magnetic Exchange Interactions in Low-Valent Manganese Alkoxide Cubes

Laura E. Pence,[1a] Andrea Caneschi,[1b] and Stephen J. Lippard*[,1a]

Department of Chemistry, Massachusetts Institute of Technology, Cambridge, Massachusetts 02139, and Dipartimento di Chimica, Universitá degli Studi di Firenze, Firenze, Italy 50144

Received November 9, 1995

In synthetic manganese chemistry, the $\{Mn_4O_4\}^{4+}$ unit has been characterized in several tetranuclear Mn(II) complexes with a single Schiff-base macrocycle encapsulating the metals to support the cube-type core.[2,3] Highly distorted Mn cubes supported by catecholate ligands have been prepared,[4] as has a cube with a $\{Mn_4Te_4\}^{4+}$ core in which all the metals are tetrahedral.[5] The $\{Mn_4O_4\}^{4+}$ cube is also encountered as a building block about which higher nuclearity structures are constructed, for example, $[Mn_8Fe_4O_{12}(O_2CMe)_{16}(H_2O)_4]$[6,7] and $[Mn_{12}O_{12}(O_2CPh)_{16}(H_2O)_4]$.[8] In both cases, the cube is assembled during cluster synthesis.

In the present note, we describe the synthesis and properties of two new examples of manganese alkoxide cubes, $[Mn(DPM)(OMe)(MeOH)]_4$, **1**, and $[Mn(DBM)(OMe)(MeOH)]_4$, **3**, where HDPM is dipivaloylmethane and HDBM is dibenzoylmethane, as well as additional characterization of $[Mn_4(DPM)_4(OEt)_4(EtOH)_2]$, **2**. The synthesis and structure of compound **2** were reported previously.[9] Both methoxide cubes contain four octahedrally coordinated manganese atoms, in contrast to the ethoxide complex, where two of the four metal atoms are only pentacoordinate. A detailed analysis of the magnetic properties of **1**−**3** was undertaken, and a general scheme was obtained which fits the χ vs T data for all three compounds, despite the structural differences among them. The previously noted instability of the cubes in solution[9] was further investigated by spectroscopic methods and fast atom bombardment (FAB) mass spectrometry.

Experimental Section

Synthetic Procedures. $MnCl_2$, HDPM, HDBM, and a 1.6 M solution of BuLi in hexanes were obtained from Aldrich and used as received. Experiments were carried out under an inert atmosphere of dry nitrogen by using standard glovebox or Schlenk-line techniques. All solvents were distilled from appropriate drying agents under a nitrogen atmosphere prior to use. $[Mn_4(DPM)_4(OEt)_4(EtOH)_2]$, **2**, was prepared as previously described.[9]

Synthesis of [Mn(DPM)(OMe)(MeOH)]$_4$ (1). A sample of anhydrous $MnCl_2$ (0.100 g, 0.795 mmol) dissolved in 1.0 mL of MeOH was added to 0.146 g (0.795 mmol) of neat HDPM. LiOMe was formed by addition of 1.0 mL of a 1.6 M solution of BuLi in hexanes to 10 mL of MeOH (1.59 mmol, 2 equiv). The two solutions were combined and agitated, and a yellow precipitate formed immediately. The microcrystalline solid was collected in quantitative yield by vacuum filtration, leaving a colorless filtrate. The product was recrystallized from toluene/methanol (yield ∼70%). Anal. Calcd for $C_{52}H_{104}O_{16}Mn_4$: C, 51.83; H, 8.70. Found: C, 51.90; H, 8.67. Electronic spectrum in 90% toluene/10% MeOH: $\lambda_{max} = 302$ nm ($\epsilon = 46\,000$ M^{-1} cm^{-1}). FTIR (KBr, cm^{-1}): 3339 (s, br), 2959 (s), 2920 (s), 2871 (s), 2836 (w), 2807 (s), 1591 (vs), 1576 (vs), 1537 (vs), 1506 (vs), 1452 (vs), 1414 (vs, br), 1389 (vs, br), 1357 (vs), 1280 (m), 1266 (m), 1246 (m), 1186 (s), 1135 (s), 1038 (vs), 956 (w), 934 (w), 868 (s), 821 (w), 791 (m), 760 (m), 739 (m), 607 (m), 475 (s).

Synthesis of [Mn(DBM)(OMe)(MeOH)]$_4$ (3). Two solutions were prepared, one containing 0.100 g of $MnCl_2$ (0.795 mmol) in 1.0 mL of MeOH and a second containing 0.146 g of HDBM (0.795 mmol) in 1.0 mL of MeOH. The latter was warmed gently to complete dissolution. The two solutions were combined with LiOMe, prepared as described above, to form an orange-red solution. Pumping on the solution briefly initiated precipitation, and the product was collected by vacuum filtration. The wet solid was redissolved in a minimum volume of either toluene or THF, the solution was filtered, and MeOH was layered over the filtrate to induce crystallization. Deep red crystals of the product formed, usually with a pale orange powder adhering to the crystals. The yield was ∼51%. Anal. Calcd for $C_{75}H_{80}O_{16}Mn_4$, **3**·toluene: C, 61.82; H, 5.53. Found: C, 61.58; H, 5.57. Electronic spectrum in 90% toluene/10% MeOH: $\lambda_{max} = 354$ nm ($\epsilon = 98\,000$ M^{-1} cm^{-1}). FTIR (KBr, cm^{-1}): 3265 (w, br), 3061 (w), 3029 (w), 2938 (w), 2920 (w), 2881 (w), 2809 (w), 1600 (s), 1556 (s), 1518 (s), 1479 (s), 1457 (s), 1404 (s, br), 1382 (s, br), 1306 (s), 1283 (s), 1223 (s), 1180 (m), 1155 (w), 1116 (w), 1071 (m), 1034 (vs), 1001 (w), 939 (m), 843 (w), 811 (w), 784 (m), 759 (s), 752 (s, sh), 722 (vs), 691 (vs), 619 (vs), 518 (m), 465 (w), 445 (w).

X-ray Crystallography. Crystalline samples of **1** and **3**·MeOH·THF were inspected by microscopy on a cold stage, mounted with grease on the end of a quartz fiber, and studied on a CAD4 diffractometer equipped with graphite-monochromatized Mo K$\bar{\alpha}$ radiation ($\bar{\lambda} = 0.710\,73$ Å). Data collection and structure refinement followed standard procedures in our laboratory,[10] details of which are reported in Table 1.

[Mn(DPM)(OMe)(MeOH)]$_4$ (1). X-ray quality-crystals of **1** were grown by layering methanol on a solution of the compound in toluene. A yellow block of approximate dimensions 0.48 × 0.36 × 0.28 mm was chosen and judged to be of acceptable quality for data collection by several ω scans having $\Delta\bar{\omega}_{1/2} = 0.237°$. The monoclinic symmetry was confirmed by axial photographs. Three periodically monitored intensity check reflections displayed no decay. The structure was solved by using the teXsan software package.[11] The four metals as well as most of the non-hydrogen atoms were located in the initial structure solution by using the program, SIR-92.[12] The rest of the structure was revealed by alternating least-squares refinement cycles and difference Fourier maps. All non-hydrogen atoms were refined anisotropically. The hydrogen atoms on the methanol oxygens were located from the difference maps; all other hydrogens were included in calculated positions. Examination of an ORTEP diagram of the refined structure revealed an elongated ellipsoid for C(5) of a methanol ligand, suggesting disorder. Further analysis of the electron density maps in this region of space resulted in a model for the disorder consisting of two carbon positions in a ratio of 2:1. The largest peak in the final difference map was 0.40 e/Å^3.

[Mn(DBM)(OMe)(MeOH)]$_4$·MeOH·THF (3·MeOH·THF). Large X-ray-quality crystals of **3** were grown from vapor diffusion of MeOH into a solution of the compound in THF. A red-orange block of approximate dimensions 0.30 × 0.40 × 0.45 mm was chosen and examined as above. The quality of the specimen was verified by ω

(1) (a) Massachusetts Institute of Technology. (b) Universitá degli Studi di Firenze.
(2) McKee, V.; Shepard, W. B. *J. Chem. Soc., Chem. Commun.* **1985**, 158.
(3) Brooker, S.; McKee, V.; Shepard, W. B.; Pannell, L. K. *J. Chem. Soc., Dalton Trans.* **1987**, 2555.
(4) Shoner, S. C.; Power, P. P. *Inorg. Chem.* **1992**, *31*, 1001.
(5) Stephan, H.-S.; Chen, C.; Henkel, G.; Griesar, K.; Haase, W. *J. Chem. Soc., Chem. Commun.* **1993**, 886.
(6) Schake, A. R.; Tsai, H.-L.; Webb, R. J.; Folting, K.; Christou, G.; Hendrickson, D. N. *Inorg. Chem.* **1994**, *33*, 6020.
(7) Schake, A. R.; Tsai, H.-L.; de Vries, N.; Webb, R. J.; Folting, K.; Hendrickson, D. N.; Christou, G. *J. Chem. Soc., Chem Commun.* **1992**, 181.
(8) Boyd, P. D. W.; Li, Q.; Vincent, J. B.; Folting, K.; Chang, H.-R.; Streib, W. E.; Huffman, J. C.; Christou, G.; Hendrickson, D. N. *J. Am. Chem. Soc.* **1988**, *110*, 8537.
(9) Taft, K. L.; Caneschi, A.; Pence, L. E.; Delfs, C. D.; Papaefthymiou, G. C.; Lippard, S. J. *J. Am. Chem. Soc.* **1993**, *115*, 11753.
(10) Carnahan, E. M.; Rardin, R. L.; Bott, S. G.; Lippard, S. J. *Inorg. Chem.* **1992**, *31*, 5193.
(11) *TeXsan: Single Crystal Structure Analysis Software, Version 1.6c;* Molecular Structure Corp.; The Woodlands, TX, 1994.
(12) Altomare, A.; Cascarano, G.; Giacovazzo, C.; Guagliardi, A.; Burla, M. C.; Polidori, G.; Camalli, M. *J. Appl. Crystallogr.* **1994**, *27*, 435.

S0020-1669(95)01448-0 CCC: $12.00

Table 1. Experimental Details of the X-ray Diffraction Studies[a] of $[Mn(DPM)(OMe)(MeOH)]_4$ (**1**) and $[Mn(DBM)(OMe)(MeOH)]_4 \cdot MeOH \cdot THF$ (**3**·MeOH·THF)

	1	**3**·MeOH·THF
formula	$C_{52}H_{104}Mn_4O_{16}$	$C_{73}H_{84}Mn_4O_{18}$
fw	1204.31	1469.21
space group	$P2_1/n$	$P\bar{1}$
a, Å	13.156(2)	13.473(2)
b, Å	31.945(6)	15.015(2)
c, Å	16.037(2)	21.071(3)
α, deg		72.620(9)
β, deg	93.57(2)	87.14(1)
γ, deg		63.62(1)
V, Å^3	6719(2)	3627.2(9)
Z	4	2
T, °C	−110	−110
ρ_{calcd}, g cm^{-3}	1.191	1.345
transm factor range	0.917−1.000	0.920−1.000
linear abs coeff, cm^{-1}	7.893	7.481
R, R_w[b]	0.045, 0.051	0.049, 0.062

[a] Data collected on an Enraf-Nonius CAD4-F geometry diffractometer with graphite-monochromatized Mo Kα̅ radiation ($\bar{\lambda}$) = 0.710 73 Å). [b] $R = \sum||F_o| - |F_c||/\sum|F_o|$; $R_w = [\sum w(|F_o| - |F_c|)^2/\sum w|F_o|^2]^{1/2}$, where $w = 4F^2/\sigma^2(F^2)$ and $\sigma^2(F^2) = [S^2(C + 4B) + (pI)^2]/(Lp)^2$ with S = scan rate, C = peak counts, B = sum of left and right background counts, I = reflection intensity, Lp = Lorentz−polarization factor, and p is a constant employed to avoid overweighting of intense reflections.

scans, for which $\Delta\bar{\omega}_{1/2}$ was 0.247°. Although the transmission factor range was small (Table 1), an empirical absorption correction was applied. The teXsan software package was used to solve the structure.[11] The metal atoms and most of the inner coordination sphere were revealed by the SHELXS-86 structure solution program.[13] The remaining atoms were located by initial DIRDIF[14] cycles followed by alternating least-squares refinement and difference Fourier maps. The lattice included two solvent molecules of crystallization. A THF molecule refined well at full occupancy, and the second region of electron density was best fit as a single methanol disordered over two sites, judging by bond distances and thermal parameters. Other than the atoms of this disordered group, all non-hydrogen atoms were refined anisotropically. Hydrogen atoms on the carbons of the cluster and the lattice THF were included at calculated positions. The maximum residual electron density was 0.8 e/Å^3 in the final difference map.

Physical Measurements. Fourier transform infrared spectra were recorded on a Bio-Rad SPC3200 instrument. UV−visible spectra were collected on either a Perkin-Elmer Lambda 7 or a Hewlett Packard 8452A diode array spectrophotometer. Solid-state magnetic measurements of **1**−**3** were made by using a Quantum Design SQUID susceptometer. More than 50 data points between 5 and 300 K were collected at 3 kG. The magnetism of the sample holders was measured at the same fields and temperatures and subtracted from the experimental values. Diamagnetic corrections were calculated from Pascal's constants and applied.[15] The standard MINUIT routine of minimization in the CLUMAG program was used to calculate the 1296 spin states.[16] Positive ion FAB mass spectra were collected at low resolution on a Finnegan 8200 mass spectrometer with an Ion Tech fast atom bombardment unit. The matrix used was 3-nitrobenzyl alcohol, and contact with air was minimized.

Results and Discussion

Synthesis and Solution Properties. The syntheses of **1**−**3** take advantage of the ability of alkoxides to bridge metal ions, forming condensed structures. The particular synthetic strategy of using base to deprotonate the alcohol and β-diketone ligands has been demonstrated previously for Mn, Fe, Co, and Ni.[9,17−19] Divalent tetranuclear cubes are known for a number of transition and alkaline earth metals with various bridging and terminal ligands.[3,4,9,19−21] Since the π-donor capability of the hard RO^- group generally produces the most stable compounds for metals in their higher oxidation states,[22] low-valent species are usually sensitive to dioxygen.[23] Such proved to be the case for **1**−**3**, which turned brown unless kept under an inert atmosphere.

Previous optical spectroscopic studies of $[Fe(L)(OMe)(MeOH)]_4$ cubes[9] revealed time-dependent changes unless a small amount of the alcohol was present in solution. The manganese analogues displayed similar shifts in their absorption maxima over time when dissolved in pure toluene, THF, or CH_2Cl_2. Spectra were therefore measured in a solution of the primary solvent containing 10% alcohol, conditions under which the compounds obeyed Beer's law. Their pale yellow and orange colors are typical of high-spin d^5 Mn(II).[24,25] The FAB mass spectra of **1** and **3** provide more direct information about the lability of the alcohol ligands. Both spectra displayed no parent ions, nor did they contain peaks attributable to $\{MnL(OMe)\}_4$ fragments. The most significant high-mass peaks occurred at 1383 amu for **1** and 1544 amu for **3**, values which can be explained by postulating reactions with the matrix prior to measuring the spectra. In particular, both high-mass peaks correspond to $[Mn_4L_4(OMe)_4(NBA)_2]H^+$ species, where NBA is 3-nitrobenzyl alcohol present as the matrix. This stoichiometry, with only two alcohols, is the same as that observed for the ethanol cube, **2**, suggesting that methanol is the only alcohol small enough to support a structure containing four six-coordinate Mn(II) centers.

Description of the Structures. Selected average bond distances and angles are presented in Table 2, and Figures 1 and 2 display ORTEP views of **1** and **3**, respectively. Both compounds have a cuboidal $\{Mn_4(OR)_4\}^{4+}$ core with manganese and oxygen atoms occupying alternate vertices. In addition to three bridging ligands, each manganese atom is coordinated to a chelating β-diketonate and a single solvent molecule to complete an octahedral coordination environment. The framework of the cubes is reinforced by the presence of hydrogen bonds between the coordinated methanols and the oxygen atom of a β-diketonate ligand (L) bound to an adjacent metal atom

(13) Sheldrick, G. M. In *Crystallographic Computing*; Sheldrick, G., Krüger, C., Goddard, R., Eds.; Oxford University Press: Oxford, U.K., 1985; p 175.
(14) Pathasarathi, V.; Beurskens, P. T.; Slot, H. J. B. *Acta Crystallogr.* **1983**, *A39*, 860.
(15) Carlin, R. L. *Magnetochemistry*; Springer-Verlag: New York, 1986. (b) O'Connor, C. J. *Prog. Inorg. Chem.* **1982**, *29*, 203.
(16) The locally written program CLUMAG takes advantage of the irreducible tensor operators method. See also: Gatteschi, D.; Pardi, L. *Gazz. Chim. Ital.* **1993**, *123*, 231.
(17) Bertrand, J. A.; Ginsberg, A. P.; Kaplan, R. I.; Kirkwood, C. E.; Martin, R. L.; Sherwood, R. C. *Inorg. Chem.* **1971**, *10*, 240.
(18) Andrew, J. E.; Blake, A. B. *J. Chem. Soc. A* **1969**, 1456.
(19) Halcrow, M. A.; Sun, J.-S.; Huffman, J. C.; Christou, G. *Inorg. Chem.* **1995**, *34*, 4167.
(20) For examples, see the following. (a) Co: Olmstead, M. M.; Power, P. P.; Sigel, G. A. *Inorg. Chem.* **1988**, *27*, 580. (b) Co: Dimitrou, K.; Folting, K.; Streib, W. E.; Christou, G. *J. Chem. Soc., Chem. Commun.* **1994**, 1385. (c) Co, Ni: Paap, F.; Bouwman, E.; Driessen, W. L.; de Graaff, R. A. G.; Reedijk, J. *J. Chem. Soc., Dalton Trans.* **1985**, 737. (d) Ni: Halcrow, M. A.; Huffman, J. C.; Christou, G. *Angew. Chem., Int. Ed. Engl.* **1995**, *34*, 889. (e) Ni: Gladfelter, W. L.; Lynch, M. W.; Schaefer, W. P.; Hendrickson, D. N.; Gray, H. B. *Inorg. Chem.* **1981**, *20*, 2390. (f) Ni: Boyd, P. D. W.; Martin, R. L.; Schwarzenbach, G. *Aust. J. Chem.* **1988**, *41*, 1449. (g) Ni: Bertrand, J. A.; Marabella, C.; Vanderveer, D. G. *Inorg. Chim. Acta* **1978**, *26*, 113. (h) Ni: Ballester, L.; Coronado, E.; Gutiérrez, A.; Monge, A.; Perpiñán, M. F.; Pinilla, E.; Rico, T. *Inorg. Chem.* **1992**, *31*, 2053. (i) Cu: Mergehenn, R.; Merz, L.; Haase, W.; Allmann, R. *Acta Crystallogr.* **1976**, *B32*, 505. (j) Cu: Schwabe, L.; Haase, W. *J. Chem. Soc., Dalton Trans.* **1985**, 1909. (k) Cu: Sletten, J.; Sørensen, A.; Julve, M.; Journaux, Y. *Inorg. Chem.* **1990**, *29*, 5054.
(21) Arunasalam, V.-C.; Baxter, I.; Drake, S. R.; Hursthouse, M. R.; Malik, K. M. A.; Otway, D. J. *Inorg. Chem.* **1995**, *34*, 5295.
(22) Hubert-Pfalzgraf, L. G. *New J. Chem.* **1987**, *11*, 663.
(23) Horvath, B.; Möseler, R.; Horvath, E. G. *Z. Anorg. Allg. Chem.* **1979**, *449*, 41.
(24) Mercati, G.; Morazzoni, F.; Naldini, L.; Seneci, S. *Inorg. Chim. Acta* **1979**, *37*, 161.
(25) Sankhla, D. S.; Mathur, R. C.; Misra, S. N. *Indian J. Chem.* **1980**, *19A*, 75.

Table 2. Selected Average Bond Distances (Å) and Angles (deg) for [Mn(DPM)(OMe)(MeOH)]$_4$, **1**, and [Mn(DBM)(OMe)(MeOH)]$_4$·MeOH·THF, **3**·MeOH·THF[a]

parameter	**1**	**3**·MeOH·THF
Mn−OMe	2.172(9)	2.174(1)
Mn−O (β-diketonate)[b]	2.12(4)	2.13(3)
Mn−O in H-bond	2.160(1)	2.157(3)
Mn−O not in H-bond	2.087(1)	2.106(1)
Mn−O(H)Me	2.273(1)	2.253(9)
MeO−Mn−OMe	82(1)	82(1)
Mn−OMe−Mn	97(2)	97(3)

[a] Values in parentheses are the standard deviations in the averaged metrical parameters. [b] The β-diketonate ligands are DPM and DBM for **1** and **3**, respectively.

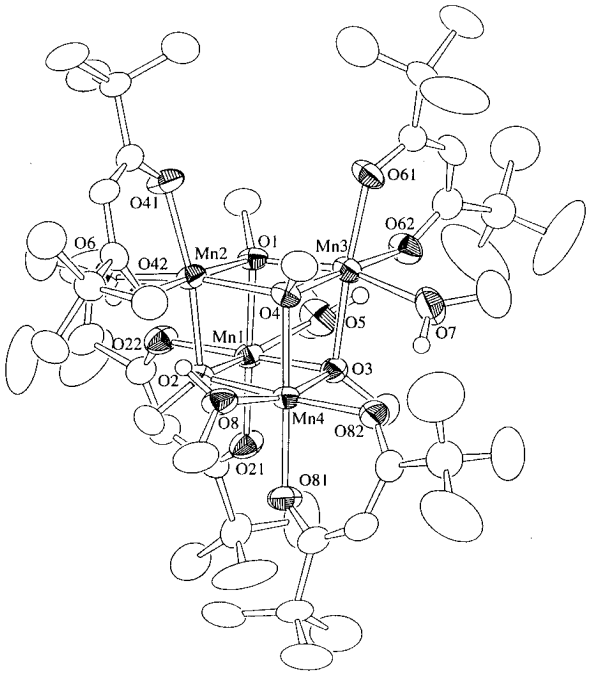

Figure 1. ORTEP diagram of [Mn(DPM)(OMe)(MeOH)]$_4$, **1**. Carbon atoms are drawn as boundary ellipsoids. All hydrogen atoms except those involved in hydrogen bonds have been omitted for clarity as well as the second orientation of the disordered methanol group.

in the cluster. The presence of these hydrogen bonds causes the Mn−O$_L$ bond to elongate to average values of 2.160(1) Å for **1** and 2.157(1) Å for **3** compared to values of 2.087(1) and 2.106(1) Å, respectively, for the β-diketonate oxygen atoms that do not participate in such hydrogen bonding. The exploitation of hydrogen bonding to enforce an ordered structure is similarly observed in hydroxide-bridged cubes, [M(CO)$_3$(μ_3-OH)]$_4$ (M = Mn, Re), where a network of intermolecular hydrogen bonds creates a superdiamondoid lattice.[26,27]

The cubes deviate slightly from ideal geometry. The internal cube angles (RO−Mn−OR) at the metal vertices average 82(1)° for both compounds whereas the comparable angles at the alkoxide corners (Mn−OR−Mn) are much larger, averaging 97(2) and 97(3)° for **1** and **3**. Since the presence of only four alcohol ligands limits the number of hydrogen bonds to 4, there are two faces across which no such interactions occur. These faces contain elongated average M−M distances of 3.31(1) and 3.31(4) Å for **1** and **3** compared to 3.231(8) and 3.24(1) Å for the faces which are spanned by a hydrogen bond (Table 3). Although the structures of the present Mn(II) cubes are isomorphous with the Fe(II) analogues having the same

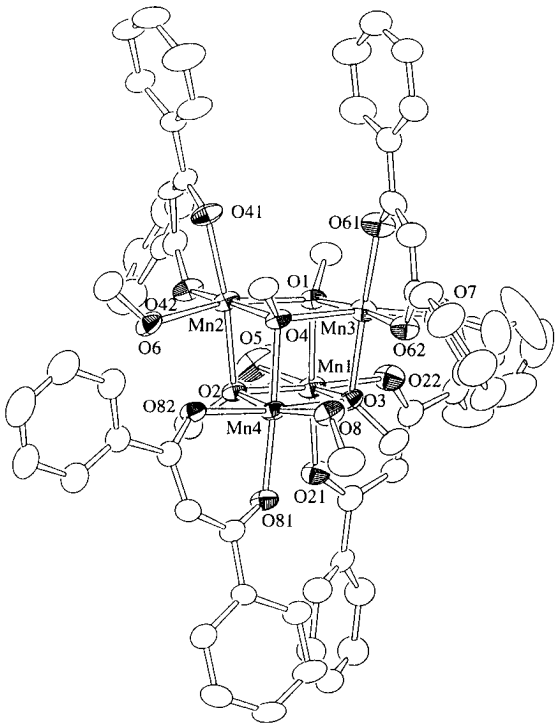

Figure 2. ORTEP diagram of [Mn(DBM)(OMe)(MeOH)]$_4$·MeOH·THF, **3**·MeOH·THF. Carbon atoms are drawn as boundary ellipsoids, and hydrogen atoms have been omitted for clarity.

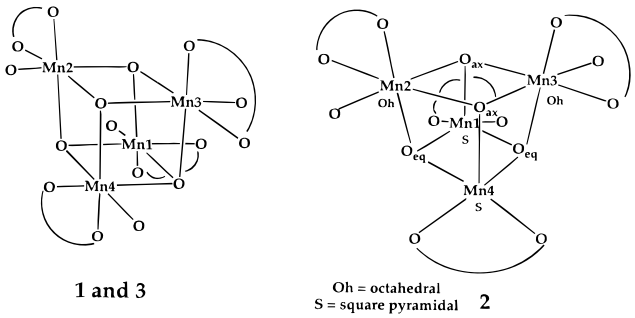

Figure 3. Schematic diagram of the two different cube stoichiometries.

Table 3. Metal−Metal Distances (Å) in [Mn(DPM)(OMe)(MeOH)]$_4$, **1**, [Mn$_4$(DPM)$_4$(OEt)$_4$(EtOH)$_2$], **2**, and [Mn(DBM)(OMe)(MeOH)]$_4$·MeOH·THF, **3**·MeOH·THF

vector	**1**	**2**[9]	**3**
Mn(2)−Mn(3)	3.3175(9)	3.351(1)	3.349(1)
Mn(1)−Mn(4)	3.2966(9)	3.277(1)	3.284(1)
Mn(1)−Mn(2)	3.2359(9)	3.225(1)	3.218(1)
Mn(1)−Mn(3)	3.2222(9)	3.147(1)	3.246(2)
Mn(2)−Mn(4)	3.2396(9)	3.156(1)	3.249(1)
Mn(3)−Mn(4)	3.2259(9)	3.227(1)	3.249(2)

composition,[9] the ethanol cube, **2**, is more distorted (Table 3 and Figure 3). The latter contains only two coordinated alcohol ligands. The resulting pentacoordinate geometry for two of the Mn(II) centers is unusual, but not unprecedented.[28−30]

Magnetic Studies. Temperature-dependent magnetic susceptibility data were obtained at 3 kG for **1**−**3** over the temperature range $5 < T < 300$ K. All three compounds display antiferromagnetic exchange coupling previously encountered for Mn(II) clusters bridged by an oxygen donor ligand.[31−35] The

(26) Copp, S. B.; Subramanian, S.; Zaworotko, M. J. *J. Chem. Soc., Chem. Commun.* **1993**, 1078.
(27) Copp, S. B.; Subramanian, S.; Zaworotko, M. J. *J. Am. Chem. Soc.* **1992**, *114*, 8719.
(28) Belforte, A.; Calderazzo, F.; Zanazzi, P. F. *J. Chem. Soc., Dalton Trans.* **1988**, 2921.
(29) Delaunay, J.; Hugel, R. P. *Inorg. Chem.* **1986**, *25*, 3957.
(30) Phillips, F. L.; Shreeve, F. M.; Skapski, A. C. *Acta Crystallogr.* **1976**, *B32*, 687.
(31) Yu, S.-B.; Lippard, S. J.; Shweky, I.; Bino, A. *Inorg. Chem.* **1992**, *31*, 3502.

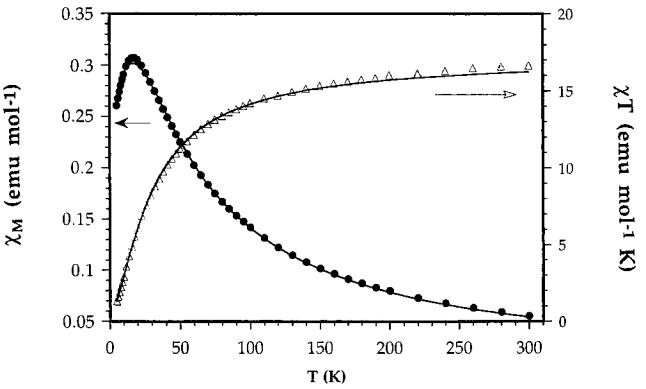

Figure 4. Temperature-dependent molar susceptibility (●) and χT plot (△) for **1** at 3000 G. The solid lines represent the best fit to the data as described in the text.

room-temperature χT values are 16.7, 17.6, and 17.4 emu mol^{-1} K (μ_{eff} = 11.5 for **1** and 11.8 μ_B for **2** and **3**), close to the expected value of χT = 17.5 emu mol^{-1} K for four $S = {}^5/_2$ uncoupled spins with $g = 2$. The χT product decreases steadily with decreasing temperature, whereas a maximum in the χ versus T plot is observed at 18 K for **1** and at 16 K for **2** and **3**, as shown respectively in Figure 4 and in Figures S1 and S2 (Supporting Information). Since the spin carriers are all d^5 Mn(II) ions, and therefore orbital singlet (S) ions, only the isotropic part of the exchange interaction was considered and the contribution of the zero-field splitting was neglected.

Within the core of each cluster, the Mn atoms occupy alternating vertices of the $\{Mn_4O_4\}^{4+}$ cube. The resulting manganese tetrahedron, with six Mn···Mn interactions, was therefore chosen to approximate the spin topology. The case of four antiferromagnetically interacting spins occupying the vertices of a regular tetrahedron is a well-known example of spin frustration. On each triangular side, two spins may align antiparallel, but the third cannot be simultaneously antiparallel to each of the others, preventing the antiferromagnetic interaction from being fully satisfied.

When a symmetrical spin Hamiltonian, $H = \sum_{i,j(i=j)} J(\mathbf{S}_i\mathbf{S}_j)$, with all coupling constants assumed to be equal, was applied, the maximum in χ could not be reproduced. To find a more accurate, less symmetrical Hamiltonian, the geometry of the clusters was examined to identify similar exchange interactions that could be grouped together. Schematic diagrams of the cubes are shown in Figure 3. Their geometry suggested the use of the spin Hamiltonian given in eq 1. In the more distorted

$$H = J_1[\boldsymbol{S}_1\boldsymbol{S}_4 + \boldsymbol{S}_2\boldsymbol{S}_3] + J_2[\boldsymbol{S}_1\boldsymbol{S}_2 + \boldsymbol{S}_1\boldsymbol{S}_3 + \boldsymbol{S}_2\boldsymbol{S}_4 + \boldsymbol{S}_3\boldsymbol{S}_4] \quad (1)$$

cluster **2**, at least four different sets of M−M distances could be identified.

Although **3** contains four octahedral metals and four hydrogen bonds, like **1**, there is less similarity both in the two long distances, 3.329(2) and 3.285(1) Å, and in the shorter metal−metal distances, 3.219(1)−3.250(2) Å. These structural differences proved to be unimportant, however, and the above Hamiltonian was used to fit the data effectively for each of the three compounds. J_1 was attributed to the two longer contacts and J_2 to the four shorter ones (Figure 5).

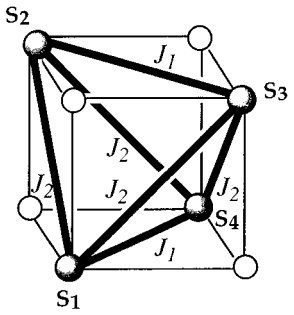

Figure 5. Assignment of J values to Mn−Mn interactions for the best magnetic model with two coupling constants for **1**−**3**.

As shown in Figures 4, S1, and S2, this model with two coupling constants allows the maxima in χ to be effectively reproduced with the following parameters: compound **1**, J_1 = 4.11, J_2 = 0.22 cm^{-1}, g = 1.99; compound **2**, J_1 = 3.88, J_2 = 0.72 cm^{-1}, g = 2.06; compound **3**, J_1 = 3.74, J_2 = 0.61 cm^{-1}, g = 2.05. The parameters are very similar for the three compounds; the differences in g cannot be considered significant since this parameter takes into account most of the experimental artifacts. When a spin Hamiltonian with three different coupling constants was employed to represent more accurately the geometries of cubes **2** and **3**, no significant improvement of the fits was obtained.

Unique attribution of the exchange coupling constants to specific pairs of metal ions is not possible owing to the high symmetry of the clusters and the intrinsic correlation of the parameters, but we prefer the set of parameters presented since it does not require unusually strong ferromagnetic interactions. Small ferromagnetic interactions up to 0.2 cm^{-1} have been observed previously in Mn(II) systems, but only in dinuclear Mn(II) systems where the ions are bridged by two phenoxo groups and the Mn(II) coordination is a slightly distorted square pyramid[36] and in a cyclic tetranuclear complex with four syn/anti carboxylate bridges.[37] In **2**, although the pentacoordinate ions, Mn(1) and Mn(4), are in a square pyramidal environment, the coordination geometry does not significantly influence the magnetic properties, which are very similar to those of **1** and **3**.[25] The antiferromagnetic exchange in the present compounds is similar to that previously reported (1.5−2.5 cm^{-1}) for a Mn(II) ion in a distorted trigonal bipyramid geometry interacting with Mn(II) in a pseudooctahedral coordination environment mediated by one phenoxo and two acetato bridges.[33,38]

Acknowledgment. This work was supported by a grant from the National Science Foundation. We thank Li Li at the MIT Chemistry Spectrometry Laboratory for measuring the FAB mass spectra, Kingsley Taft for advice, and Susanna Herold and Joanne Yun for helpful comments on the manuscript. L.E.P. is grateful to the National Institutes of Health for a National Research Service Award (CA-59223).

Supporting Information Available: An expanded table of X-ray experimental details and, for non-H atoms, complete listings of atomic coordinates, anisotropic thermal parameters, bond lengths, and bond distances for complexes **1** and **3**, as well as magnetic susceptibility plots for **2** and **3** (27 pages). Ordering information is given on any current masthead page.

IC951448H

(32) Rardin, R. L.; Poganiuch, P.; Bino, A.; Goldberg, D. P.; Tolman, W. B.; Liu, S.; Lippard, S. J. *J. Am. Chem. Soc.* **1992**, *114*, 5240.
(33) Higuchi, C.; Sakiyama, H.; Okawa, H.; Isobe, R.; Fenton, D. E. *J. Chem. Soc., Dalton Trans.* **1994**, 1097.
(34) Kessissoglou, D. P.; Butler, W. M.; Pecoraro, V. L. *Inorg. Chem.* **1987**, *26*, 495.
(35) Brooker, S.; McKee, V. *J. Chem. Soc., Chem. Commun.* **1989**, 619.
(36) Luneau, D.; Savariault, J.-M.; Cassoux, P.; Tuchagues, J.-P. *J. Chem. Soc., Dalton Trans.* **1988**, 1225.
(37) Jiang, Z.-H.; Ma, S.-L.; Liao, D.-Z.; Yan, S.-P.; Wang, G.-L.; Yao, X.-K.; Wang, R.-J. *Sci. China, Ser. B* **1994**, *37*, 923.
(38) Sakiyama, H.; Tamaki, H.; Kodera, M.; Matsumoto, N.; Okawa, H. *J. Chem. Soc., Dalton Trans.* **1993**, 591.